Calcium Waves Induced by Large Voltage Pulses in Fish Keratocytes

Ingrid Brust-Mascher and Watt W. Webb
School of Applied and Engineering Physics, Cornell University, Ithaca, New York 14853 USA

ABSTRACT Intracellular calcium waves in fish keratocytes are induced by the application of electric field pulses with amplitudes between 55 and 120 V/cm and full width at half-maximum of 65–100 ms. Calcium concentrations were imaged using two-photon excited fluorescence microscopy (Denk et al., 1990. *Science.* 248:73–76; Williams et al. 1994. *FASEB J.* 8:804–813) and the ratiometric calcium indicator indo-1. The applied electric field pulses induced waves with fast calcium rise times and slow decays, which nucleated in the lamellipodium at the hyperpolarized side of the cells and, less frequently, at the depolarized side. The effectiveness of wave generation was determined by the change induced in the membrane potential, which is about half the field strength times the cell width in the direction of the field. Stimulation of waves began at voltage drops across the cell above 150 mV and saturated at voltage drops above 300 mV, where almost all cells exhibited a wave. Waves were not induced in low-calcium media and were blocked by the nonselective calcium channel blockers cobalt chloride and verapamil, but not by specific organic antagonists of voltage-sensitive calcium channel conductance. Thapsigargin stopped wave propagation in the cell body, indicating that calcium release from intracellular stores is necessary. Thus a voltage pulse stimulates Ca^{2+} influx through calcium channels in the plasma membrane, and if the intracellular calcium concentration reaches a threshold, release from intracellular stores is induced, creating a propagating wave. These observations and the measured parameters (average velocity ~66 μm/s and average rise time ~68 ms) are consistent with a wave amplification model in which

$$\nu = \sqrt{D/\tau}$$

determines the effective diffusivity of the propagating molecules, $D \approx 300\ \mu m^2/s$ (Meyer, 1991. *Cell.* 64:675–678).

INTRODUCTION

Calcium plays an important role in many cell processes. It is a second messenger in signaling pathways (Clapham, 1995), in which signaling often occurs via waves or oscillations (Clapham, 1995; Fewtrell, 1993; Meyer and Stryer, 1991; Tsien and Tsien, 1990) that may involve inositol trisphosphate, another second messenger (Berridge, 1993). In motile cells, calcium is involved in the regulation of locomotion, because the state of the actin cytoskeleton, whose structure and dynamics determine shape and motility, is defined by actin-binding proteins, many of which are calcium regulated (Forscher, 1989; Janmey, 1994; Stossel, 1989; Weeds, 1982). Although the role of calcium in motility is not well understood, it has been evidenced by several experiments. Spontaneous locomotion and electrotaxis of fish keratocytes is blocked by nonselective calcium channel blockers (Cooper and Schliwa, 1985, 1986). Calcium-permeable *Xenopus laevis* epidermal cells can be directed by local calcium release (Mittal and Bereiter-Hahn, 1985). Transient calcium increases are needed for motility of neutrophils over certain substrates (Hendey and Maxfield, 1993; Marks et al., 1991; Marks and Maxfield, 1990; Maxfield, 1993). Spatially heterogeneous calcium distributions are seen in migrating eosinophils (Brundage et al., 1991, 1993) and fibroblasts in the later stages of wound healing (Hahn et al., 1992).

The motion of several cell types can be induced and reoriented by steady electric fields (for reviews see Nuccitelli, 1988; Robinson, 1985); for example, fish keratocytes (Cooper and Schliwa, 1985, 1986), National Institutes of Health-3T3 and SV101 fibroblasts (Brown and Loew, 1994), and human keratinocytes (Nishimura et al., 1996) move toward the cathode. It has been proposed that Ca^{2+} ions play a role in the regulation of this movement, but studies on the effect of electric fields on intracellular calcium concentration ($[Ca^{2+}]_i$) have not been conclusive. Onuma and Hui (1988) reported that electric fields increase $[Ca^{2+}]_i$ in galvanotactic C3H/10T1/2 fibroblasts. Brown and Loew (1994) reported that electric field-directed locomotion in two murine fibroblastic cell lines, National Institutes of Health-3T3 and SV101, is a calcium-independent process, whereas Mullins et al. (1992) reported that extremely low-frequency sinusoidal electric fields mobilize calcium from intracellular stores in Swiss 3T3 fibroblasts.

An electric field interacts with a cell in two ways. First, it alters the membrane potential by hyperpolarizing and depolarizing the anode and cathode facing sides of the cell, respectively (Gross et al., 1986), which can modify the movement of ions across the plasma membrane. Second, it redistributes proteins on the cell surface by electroosmosis

Received for publication 20 February 1998 and in final form 11 June 1998.

Address reprint requests to Dr. Watt W. Webb, School of Applied Physics, Cornell University, 223 Clark Hall, Ithaca, NY 14853-2501. Tel.: 607-255-3331; Fax: 607-255-7658; E-mail:www2@cornell.edu.

Dr. Brust-Mascher's present address is Department of Biochemistry, University of Minnesota, Minneapolis, MN 55455.

0006-3495/98/10/1669/10 $2.00

or electrophoresis (McCloskey et al., 1984; Poo, 1981). Cell surface protein redistribution affects many cell processes; it can trigger a signaling pathway. For example, in rat basophilic leukemia cells steady electric fields induce a rise in $[Ca^{2+}]_i$ due to protein electroosmosis (Feder and Webb, 1994).

We have studied intracellular calcium distributions in fish keratocytes, which migrate spontaneously in culture and exhibit cathode-directed galvanotaxis with average speeds of 20–30 μm/min (Cooper and Schliwa, 1986), which is rapid compared with most vertebrate cells (Bray, 1992). In this paper we report that electric field pulses induce fast calcium waves in these cells, although no detectable changes were observed upon the application of small steady electric fields. The pulse-induced waves start with Ca^{2+} entry through Ca^{2+} channels in the plasma membrane and propagate by stimulation of intracellular Ca^{2+} release. The parameters measured for these waves are consistent with a simple amplification model (Meyer, 1991).

MATERIALS AND METHODS

Cell isolation and culture

Individual scales were removed from goldfish with forceps. A single scale was placed in a drop of Amphibian Culture Medium (ACM) (Gibco BRL) with 10 μl/ml gentamicin (Gibco BRL) and 15 mM HEPES (Sigma) on a sterile coverslip, covered with a second coverslip, and placed in a culture dish. After 40 min, 1.5 ml of the solution was added to the dish and the dish was sealed with parafilm. Cells were allowed to migrate onto one of the coverslips overnight. They were incubated at room temperature in Dulbecco's phosphate-buffered saline (PBS) without calcium for 20 min and returned to ACM with gentamicin and HEPES for at least 20 min before use.

Cell staining

Buffer A consists of 50% ACM and 50% Fish Ringer's (112 mM NaCl, 2 mM KCl, 2.4 mM $NaHCO_3$, 1 mM $CaCl_2$, 1 mM Tris buffer, pH 7.4) supplemented with 2 mM glucose. The loading buffer is made of buffer A with 250 μM sulfinpyrazone (Sigma), 0.015% (wt/wt) pluronic (Molecular Probes), and 1 μM indo-1-AM (Molecular Probes). The rinsing buffer is buffer A with 250 μM sulfinpyrazone. Cells were incubated in loading buffer at room temperature for 20 min, rinsed with rinsing buffer three times, and then imaged in this buffer. The intracellular dye concentration, determined by comparison with known indo-1 calibration solutions, varied between 50 and 80 μM. Experiments were performed at room temperature within 2 h of loading. In this time period the dye did not enter organelles, because cells lost all of their fluorescence upon permeabilization with the plasma membrane-specific detergent digitonin (10 mM). Microinjected indo-1-salt or indo-1-dextran showed the same distributions as indo-1-AM, also proving that there was no dye compartmentalization. At longer time periods (>3 h), punctate staining appeared, but experiments were always ended well before this.

Pharmacological treatments

To test the role of calcium channels, channel blockers were added to the imaging buffer at the following concentrations: 10 mM $CoCl_2$, 50 μM verapamil, 10–50 μM nitrendipine, 10–50 μM nicardipine, 50–100 μM bepridil, and 10 μM flunarizine. The following toxins were used: 1 μM taicatoxin, 1 μM ω-agatoxin IVA, 5 μM ω-conotoxin MVIIC, 10 μM ω-conotoxin GVIA. All toxin stock solutions were made in 0.1% BSA, 100 mM NaCl, 10 mM Tris, and 1 mM EDTA at pH 7.5. Stock solutions were diluted 1000-fold in imaging buffer with 0.01% BSA. These concentrations are higher than those needed to block the corresponding channels in other cells; no channel studies have been reported in keratocytes. At higher concentrations keratocytes were damaged; that is, cells stopped moving and changed shape. They eventually rounded up and detached from the surface. $CoCl_2$ and verapamil were from Sigma; all other channel blockers and toxins were from Alomone Labs (Israel).

To test the role of sodium channels, choline chloride and choline bicarbonate were substituted for NaCl and $NaHCO_3$ in Fish Ringer's at the same concentrations. Low-calcium saline was made by substituting $MgCl_2$ for $CaCl_2$ in Fish Ringer's; calcium contamination in the range of 200–500 nM remained. Thapsigargin (Molecular Probes) was added to the imaging buffer at 1 μM concentration. For experiments with 1,2-bis(2-aminophenoxy)ethane-*N,N,N,N*-tetraacetic acid (BAPTA), 50 μM BAPTA-AM (Molecular Probes) was added to the loading buffer, and the incubation time was increased to 25 min.

Application of electric field pulses

A coverslip with attached cells was fitted into a closed chamber made with a heat-conducting sapphire plate. The thickness of the cell space was ~150 μm. The ends of the chamber were in contact with agarose-filled (Ultrapure electrophoresis grade; Bethesda Research Labs) wells (0.6 cm deep, 5 cm long, and 1.5 or 2.5 cm wide). Platinum electrodes were at the ends of these wells to avoid contamination by reactants. A second pair of platinum electrodes was used to measure the voltage across the cell space. An electrophoresis power supply (Pharmacia Fine Chemicals) gives a large transient voltage pulse with an amplitude dependent on the resistance of the chamber. A fast oscilloscope was used to characterize each pulse. Pulse amplitudes varied between 55 and 120 V/cm, rise times between 60 and 75 ms, and decay times between 100 and 250 ms. A flash lamp was turned on simultaneously with the power supply to obtain a light marker indicating the event in the image. We can therefore correlate the start of the wave with the pulse application.

Instrumentation

We used two-photon excited fluorescence microscopy (Denk et al., 1990; Williams et al., 1994) to measure fluorescence intensities. Two-photon microscopy is a nonlinear optical technique in which each normally UV-excited fluorophore is activated by the simultaneous absorption of two red photons from a highly focused pulsed red laser. Because this process is dependent on the square of the intensity, it is much more localized to the beam focus, where the densities are highest. It thus provides ideal confocal-like signal-isolation properties without any fluorophore bleaching out of the plane of focus. This technique also allows the use of the UV-excitable indo-1, an emission ratiometric calcium indicator dye, without the complications inherent in UV confocals (chromatic aberrations, low transmissivities, special UV optical elements, etc.) (Piston et al., 1994).

Fig. 1 shows a schematic diagram of the experimental setup. Pulses (705 nm, 140–160 fs) were obtained from a femtosecond, mode-locked Ti: sapphire laser (Tsunami; Spectra-Physics) pumped by an argon ion laser (BeamLok; Spectra-Physics). This light was attenuated and guided onto the scanning mirrors of a Biorad MRC-600 confocal microscope. The beam was then directed into a Zeiss Axiovert-35 and focused onto the sample with a Zeiss 40× 1.3 NA Plan-Neofluor objective. The intensity at the sample was 3–5 mW. At this intensity there was no evidence of photodamage; cells did not change their shape or their velocity of movement during exposures up to three times our normal experimental time (10–15 min).

Because of the localized nature of two-photon excitation, the confocal spatial filtering performed by the detection pathway of the MRC-600 is no longer necessary. Thus to avoid signal degradation by extraneous optical elements, detection was done externally. The fluorescence was separated from the excitation light by a long-pass dichroic mirror (520 nm), focused,

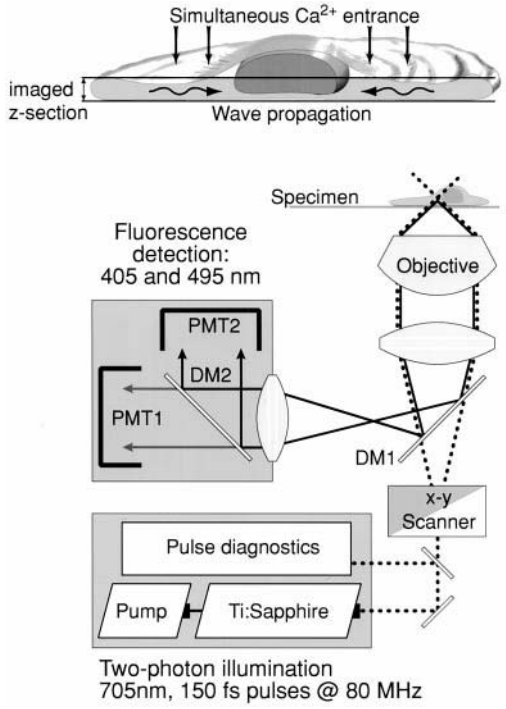

FIGURE 1 Schematic diagram of the two-photon laser scanning microscope. The incoming laser light is scanned by a Biorad MRC-600, directed into a Zeiss Axiovert-35, and focused with a Zeiss 40×, 1.3 NA Plan Neofluor objective. Fluorescence light is separated from excitation light by a long-pass dichroic mirror (DM1), focused, split by a second dichroic mirror (DM2), filtered, and monitored simultaneously by two photomultiplier tubes (PMT) placed conjugate to the back aperture of the objective. Because of the inherent confocal quality of this method, only a thin *z*-section is imaged. As shown in the inset, we position the cell so that the thin lamellipodium is completely enclosed in the imaged section.

and then split by a second dichroic mirror (450 nm) into the two emission peaks of the bound and unbound states of indo-1 (405 and 495 nm, respectively). These two signals were filtered (Omega Optical bandpass filters 405DF35 and 495DF20) and monitored simultaneously with two photomultiplier tubes (PMTs) (Hamamatsu AT7831) placed conjugate to the back aperture of the objective. Because the back aperture is a pivot point of the scanned beam, the fluorescence is stationary at the PMT, and any varying sensitivity at the photocathode does not pose a significant problem. The signals from the PMTs were amplified and sent to the external junction box of the MRC-600 interface. The regular Biorad software was used to acquire and view images.

Two-photon microscopy is inherently confocal, and the imaged *z*-section is ~1 μm thick. The lamellipodium is thinner than this; therefore we positioned the cell so that its thickness was completely enclosed in the imaged section (Fig. 1, *top*). To observe the rapid $[Ca^{2+}]_i$ responses elicited by voltage pulses, we used the line-scan mode of the confocal microscope to image a single line parallel to the direction of the field. The laser beam is repeatedly scanned in one dimension at ~12 ms per line. These lines are successively recorded, with each horizontal line added below the preceding line to form the line scan image. The vertical axis in the two-dimensional image represents time, which increases from top to bottom. This yields a time record of the $[Ca^{2+}]_i$ activity along a single line through the cell as shown in all figures.

Image pair calibrations

Images were acquired simultaneously at 405 nm and 495 nm. For analysis each pair was smoothed (3*3 kernel), background subtracted, and ratioed. A calibration look-up table was constructed from measured fluorescence intensities of 50 μM indo-1 salt in 150 mM KCl, with either saturating calcium (10 mM) or EGTA (10 mM). The conversion to absolute calcium concentrations is given by

$$[Ca^{2+}] = k_d\beta(R - R_{min})/(R_{max} - R)$$

where R is the measured ratio of fluorescence emission at 405 nm to that at 495 nm, R_{min} is the ratio in the absence of calcium, R_{max} is the ratio in the presence of saturating calcium, β is the ratio of the intensities at 495 nm in the absence and presence of calcium, and k_d = 250 nM is the indo-1 binding constant (Grynkiewicz et al., 1985).

Indo-1 may alter its spectral properties and binding constant inside cells (Blatter and Wier, 1990; Hove-Madsen and Bers, 1992); if this is the case measured calcium concentrations are not absolute, but relative changes are not affected (Bassani et al., 1995). The concentration is measured reliably if it is close to the indicator's binding constant. At concentrations such that the ratio is close to R_{min} or R_{max} (i.e., at low or high concentrations), the error in the measurement is large. The pulse-induced $[Ca^{2+}]_i$ waves reached high calcium levels, which could saturate the dye. In this case additional large differences in $[Ca^{2+}]$ do not change the fluorescence. Therefore, we can only give a lower limit for the magnitude of the wave. We studied the dynamics of induced waves; a reliable measure of their magnitude can be obtained by using an indicator with a micromolar binding constant.

RESULTS

A motile keratocyte has a distinct morphology. Its cell body, containing the nucleus and all organelles, is in the rear, and a very thin (<1 μm) lamella is extended outward in the direction of motion. Keratocytes exhibit calcium gradients with higher calcium in the cell body than in the lamellipodium, and smaller heterogeneities within the lamellipodium during turns (Brust-Mascher et al., 1994, 1995, and manuscript in preparation).

Application of a voltage pulse with an amplitude between 55 and 120 V/cm and a full width at half-maximum between 65 and 100 ms gave rise to a very fast calcium increase that propagated through the cell (Fig. 2). This response was elicited by the applied voltage pulse, because a small steady electric field (~10 V/cm), which induced electrotaxis, did not elicit this immediate calcium increase. We excluded the possibility that calcium entry was a result of electroporation (field-induced membrane perforation) of the cells by placing the cells in media with fluorescein and applying many pulses, a common method of visualizing electroporation. The dye did not enter the cells. In addition, cells did not lose indo-1 even after repeated pulse applications.

Cells exhibited a variety of responses (Fig. 2). Some cells underwent a fast, sharp $[Ca^{2+}]_i$ wave; others underwent a slow $[Ca^{2+}]_i$ rise (Fig. 2 *A*). In this case, Ca^{2+} entered the cell, but was not concentrated enough to propagate a wave. When a wave was induced, it followed the pulse with varying lag times. The anode-facing side, which is hyperpolarized, usually responded before the cathode-facing side, which is depolarized. Calcium entered the cell at the hyperpolarized side (see below for evidence of Ca^{2+} entry) while the voltage was high, around the peak of the pulse. The wave at the depolarized side started between 20 and 150 ms later, usually during the falling phase of the voltage pulse. Waves propagated from the lamellipodium into the cell

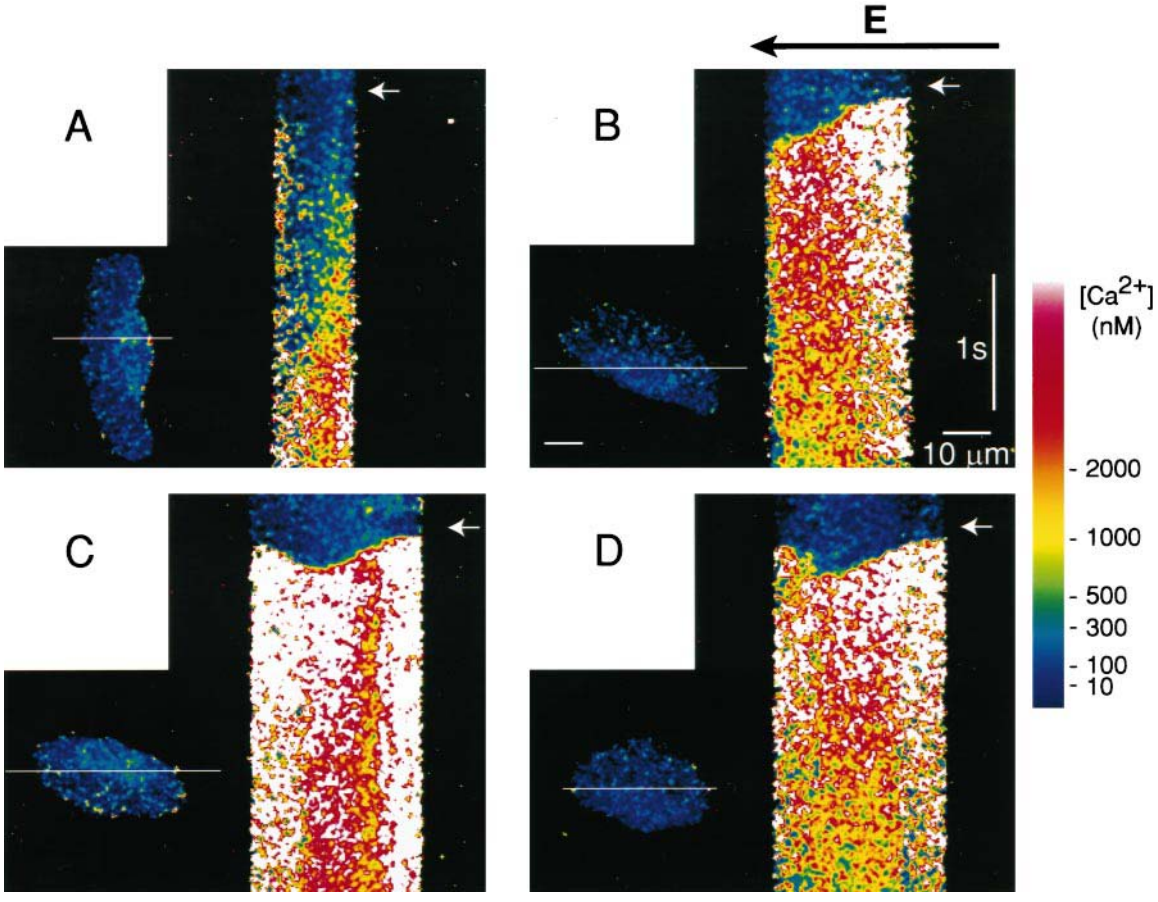

FIGURE 2 Calcium waves induced by large voltage pulses. This figure shows different examples of $[Ca^{2+}]_i$ waves, elicited by a voltage pulse of amplitude ~76V/cm. In each case, a single line through the cell, shown at left, was repeatedly scanned. The time course of $[Ca^{2+}]_i$ along this line is shown at right; time increases from top to bottom. The pulse starts at the arrow. Ca^{2+} entry always occurs at the hyperpolarized side, and often at the depolarized side tens of milliseconds later (*C* and *D*). Waves propagate through the cell body (*B*, *C*, and *D*); the average velocity (calculated from the slope of the wave front) is 66 ± 40 μm/s for waves propagating from the hyperpolarized side and 60 ± 38 μm/s for waves propagating from the depolarized side. $[Ca^{2+}]_i$ reaches micromolar concentrations with an average rise time of 68 ± 23 ms. In some cases (*A*), Ca^{2+} influx is not enough to propagate a wave. This cell is perpendicular to the field and has a smaller voltage drop across it; the effectiveness of wave generation is determined by the change induced in the membrane potential (see text and Fig. 3).

body at different speeds. $[Ca^{2+}]_i$ increased to micromolar concentrations (>3 μM).

Cells with their long axis parallel to the field experience a larger voltage drop than those with their long axis perpendicular to the field. We observed that they were also more likely to exhibit a wave, which suggests that the size of the voltage drop across the cell is an important factor in the generation of these waves. To find the threshold voltage necessary to elicit a wave, we separated the cells into three groups and assigned each group a cell response: 1) for cells in which a wave was propagated, response = 1; 2) for cells that had no wave but showed a calcium increase within 15 s, response = 0; and 3) for cells that underwent no change in calcium concentration during the observation time, response = −1. The peak applied voltage drop across the cell is the product of the applied pulse peak and the size of the cell in the direction of the field. The change induced in the membrane potential is half of this voltage drop, in which the anode-facing side is hyperpolarized and the cathode-facing side is depolarized (Gross et al., 1986).

A plot of the response as a function of the voltage drop across the cell induced by the applied pulse (Fig. 3) shows that there is a wide threshold between 150 and 300 mV. In this range, cells showed all three responses, and one cell sometimes responded differently to different pulse applications. Above this range most cells exhibited a propagating wave.

When the cells were bathed in low calcium saline, pulse application did not induce a wave. The waves were also blocked by the inorganic calcium channel blocker $CoCl_2$ and by the organic channel antagonist verapamil at a high concentration. Thus generation of a wave requires calcium entry through calcium channels in the plasma membrane. To test whether voltage-gated channels are involved, we used specific channel blockers. Voltage-gated channels are primarily found in excitable cells, although L- and T-type channels are also present in some nonexcitable cells (Tsien and Tsien, 1990). Because it is not known which, if any, voltage-gated channels are found in keratocytes, we used a series of blockers and toxins at concentrations higher than

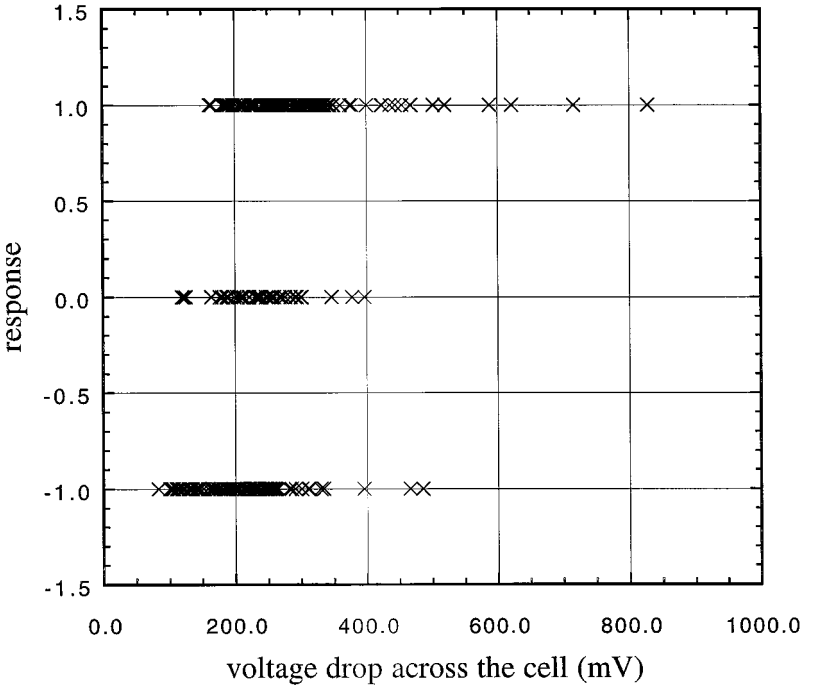

FIGURE 3 Transcellular voltage drop necessary to elicit calcium waves. This graph shows the response of individual cells as a function of the voltage drop across them. The response is defined as 1 if a wave is elicited by a pulse; 0 if the cell exhibits no wave, but its calcium increases within 15 s; and −1 if there is no change in $[Ca^{2+}]_i$ during the observation time. The voltage drop is calculated as the peak electric field multiplied by the width of the cell in the direction of the field. The potential change superimposed on the resting membrane potential is half of this voltage drop. At voltage drops between 150 and 300 mV, cells show all three responses, but above this range most cells exhibit a wave.

necessary to block the respective channels in other cells. Nicardipine, nitrendipine, and taicatoxin block L-type channels; ω-agatoxin IVA blocks P-type channels; ω-conotoxin MVIIC blocks Q-type channels; ω-conotoxin GVIA blocks N-type channels; and bepridil and flunarizine block T-type channels. Waves with the same dynamics (rise times, maximum $[Ca^{2+}]_i$, and decay times) were elicited by a voltage pulse even when these blockers were in the medium. The combination of nicardipine and ω-conotoxin GVIA or flunarizine did not abolish the waves either. Thus blocking each channel individually, and L and T-type or L and N-type channels simultaneously, did not detectably change the waves, indicating that known voltage-gated channels are probably not responsible for Ca^{2+} entry. The involvement of sodium channels is also excluded, because pulses elicited waves in a saline with sodium replaced by choline, which cannot enter the cells through sodium channels.

The waves require calcium influx through the plasma membrane. To test the role of intracellular calcium release in wave propagation, cells were treated with 1 μM thapsigargin, which blocks the intracellular CaATPase and empties intracellular stores (Thastrup, 1990). When the pulse was applied, Ca^{2+} entered the cell, usually at the hyperpolarized edge, and $[Ca^{2+}]_i$ in the lamellipodium increased rapidly, but the wave did not propagate completely through the cell body (Fig. 4). This was observed for all thapsigargin-treated cells ($n = 33$) and indicates that intracellular Ca^{2+} release is necessary for wave propagation. Therefore, the wave is generated by Ca^{2+} influx and propagated by release from intracellular stores.

Loading the cells with BAPTA, a calcium chelator, inhibited the waves, allowing only a moderate $[Ca^{2+}]_i$ increase. Ca^{2+} entered the cell, but was rapidly buffered by BAPTA, so that calcium release inside the cell was not induced, and a wave could not be propagated.

$[Ca^{2+}]_i$ usually increased simultaneously across a region of the lamellipodium. $[Ca^{2+}]_i$ increased first in the hyperpolarized region and 20–150 ms later in the depolarized one. The increase was simultaneous across each of these regions, because the lamellipodium is very thin (<1 μm) and was completely included in the imaged section. From this part of the cell the wave propagated into the cell body (Fig. 1, *top*). Here the velocity of propagation can be calculated from the slope of the wave train in the line scan images. In the cell body waves propagating from the hyperpolarized side had an average velocity of 66 ± 40 μm/s ($n = 152$) (Fig. 5). Fewer waves propagated in from the depolarized side, and the average velocity in this case was 60 ± 38 μm/s ($n = 35$). The time for $[Ca^{2+}]_i$ to reach maximum concentration can also be estimated from the line scan images (it will be underestimated if the dye saturates). The average rise time was 68 ± 23 ms.

Calcium concentrations dropped to values 30–50% above prefield values within a few seconds and returned to basal levels within a few minutes. Subsequently, many stimulated cells exhibited transient calcium increases (Fig. 6). The spikes occurred at intervals of ~2 min, and the $[Ca^{2+}]_i$ increase lasted for 20 s, the interval between images, or less. Calcium increased up to fivefold (~1 μM) from a basal level comparable to prepulse concentrations. These spikes did not reach the high $[Ca^{2+}]_i$ observed during wave propagation. Spontaneous spiking, which is not observed in unstimulated cells, could be very long lasting; in the example shown (Fig. 6) there was no decrease in the frequency or size of the transients for 25 min.

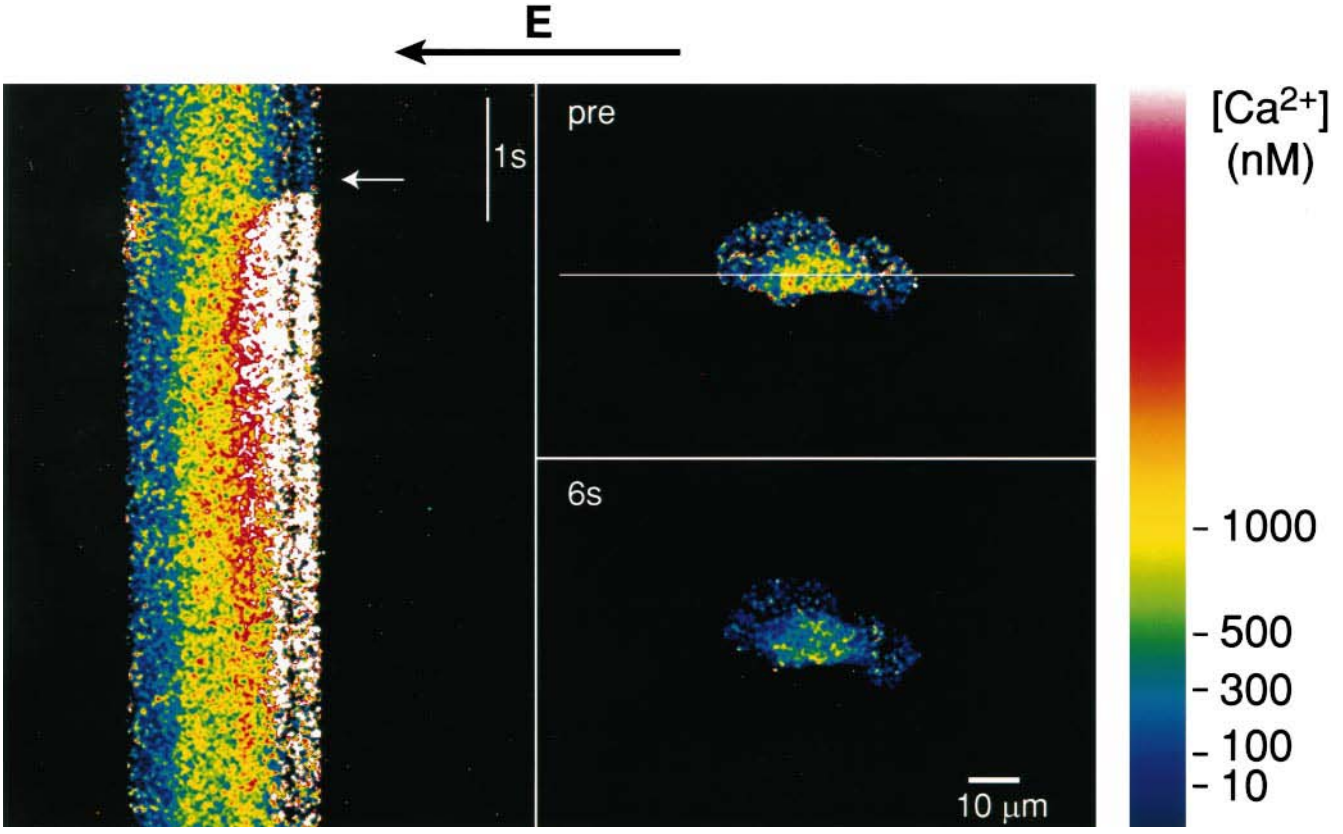

FIGURE 4 Response in a thapsigargin-treated cell. A thapsigargin-treated cell was subjected to a pulse of amplitude 72 V/cm (*line scan image at left*; the *arrow* indicates the start of the pulse). Calcium enters the cell in the lamellipodium, preferentially at the hyperpolarized side, and reaches micromolar levels, but the wave does not propagate through the cell body, thus showing that intracellular calcium release is needed for wave propagation. Pre and post images are shown at right.

After 1–2 min, application of another pulse elicited a new wave. Cells were stimulated repeatedly without detectable damage. They did not change their shape and were still electrotactic; if a small steady electric field of ~10 V/cm was applied after pulse application, the cells oriented and migrated toward the cathode, as before pulse stimulation. Cells also oriented toward the cathode after repeated pulse applications less than 2 min apart.

DISCUSSION

The application of an electric field pulse induces a $[Ca^{2+}]_i$ wave in fish keratocytes, which are electrotactic. Calcium enters the cell through the plasma membrane, and a calcium wave is propagated by stimulation of intracellular calcium release. The propagation velocities are relatively high, falling into the upper range of observed calcium waves (Jaffe, 1991).

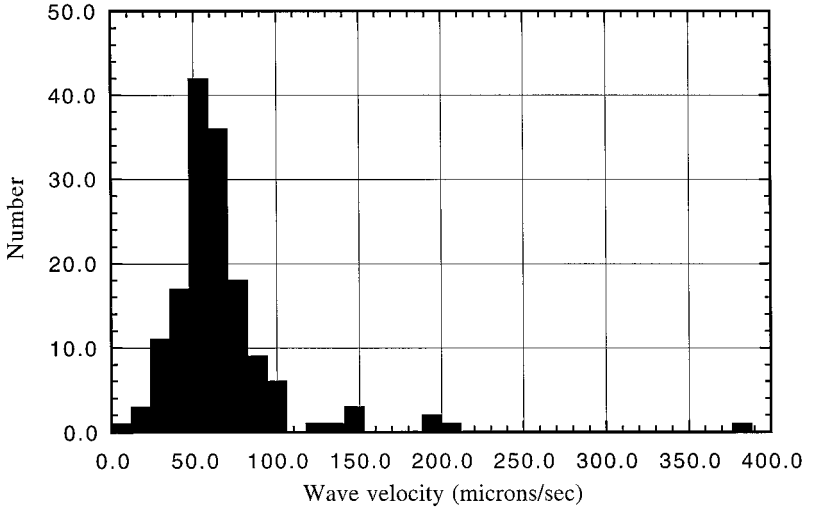

FIGURE 5 Wave velocity in the cell body. This histogram shows the distribution of velocities for waves propagating through the cell body starting at the hyperpolarized side, the primary side for wave initiation. The average velocity is 66 ± 40 μm/s (n = 152).

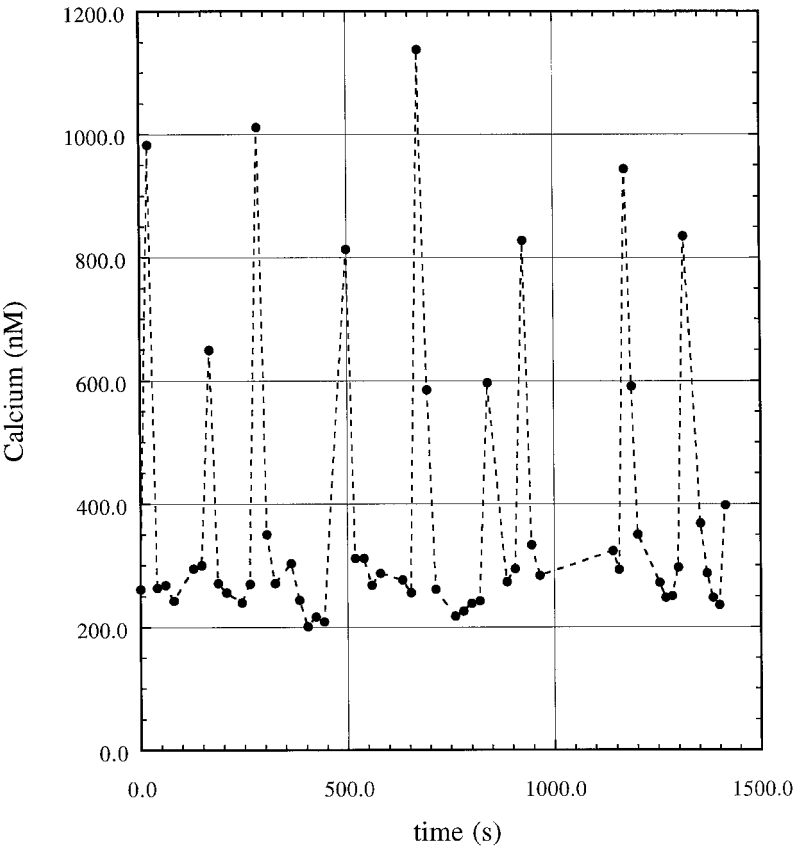

FIGURE 6 Transient calcium increases subsequent to pulse application. Average calcium concentrations in the cell body for a typical cell are shown as a function of time, sampled at ~20-s intervals after pulse stimulation. Spontaneous calcium spikes appear at ~2-min intervals. The basal $[Ca^{2+}]_i$ (~250 nM) is comparable to that before pulse application; calcium increases up to fivefold during each transient. Calcium spikes usually occur simultaneously in the lamellipodium.

Wave initiation

The induced wave starts with Ca^{2+} influx through the plasma membrane. This influx does not appear to be a result of electroporation. The applied pulses of electric field created a voltage drop of 50–250 mV across the plasma membrane superimposed on the resting membrane potential. The potential required for electrical breakdown is ~1 V across the membrane (Ghosh et al., 1993; Zimmermann, 1982), which is 3–10 times larger than the induced potential. Electroporation is generally visualized by uptake of foreign molecules (Ghosh et al., 1993; Prausnitz et al., 1994). We placed the cells in a medium with a high concentration of fluorescein and applied many pulses; fluorescein did not enter the cells. In addition, indo-1 did not leak out of the cells, because the fluorescence intensity did not decrease after repeated pulse applications. Thus electroporation is unlikely to be responsible for Ca^{2+} influx; if it is occurring, the pores must be smaller than 0.6 nm to prevent leakage of indo-1 and uptake of fluorescein.

Stimulated calcium influx occurs through channels in the plasma membrane, because it is blocked by the nonspecific calcium channel blockers $CoCl_2$ and verapamil. The affected channels are probably not voltage-gated, because the stimulated waves were not affected by the application of blockers specific for these channels, although we cannot exclude the possibility of unknown voltage-gated channels insensitive to the series of blockers and toxins used. We used the highest concentrations that would not produce detectable changes in keratocytes. These are more than enough to block these channels in cells in which they have been studied. Different types of channels exist in various cell types, including ligand-gated receptor channels, nonselective stretch-activated channels, depletion-activated channels (Lückhoff and Clapham, 1994; Parekh et al., 1993; Putney, 1990; Randriamampita and Tsien, 1993), and nonselective cation channels. Neutrophils have Ca^{2+}-activated nonselective cation channels that are highly permeable to Ca^{2+} (von Tscharner et al., 1986).

The presence of such Ca^{2+}-activated channels in keratocytes (as yet undetected) would explain wave propagation within the lamellipodium, because a small Ca^{2+} influx can be amplified through such channels. Calcium entry generally started at the hyperpolarized side, which has an enhanced electrical component of the electrochemical gradient for Ca^{2+}. $[Ca^{2+}]_i$ is on the order of 100 nM, and the extracellular $[Ca^{2+}]$ is 1 mM; thus the Nernst potential for Ca^{2+} is ~116 mV. With a resting potential of ~−50 mV, the driving force will be ~170 mV. During pulse application the membrane potential was hyperpolarized to ~−100 to ~−300 mV; in this case the driving force increases to ~200–420 mV. This increase is probably enough to drive significant Ca^{2+} influx through Ca^{2+}-permeable channels in the plasma membrane.

This is consistent with the observation that some cells enhance Ca^{2+} entry by hyperpolarization. Voltage-independent Ca^{2+}-selective channels triggered by second messen-

gers allow Ca^{2+} entry, which is increased when the cell is hyperpolarized by open K^+ channels (Clapham, 1995). Externally applied hyperpolarization increases Ca^{2+} entry in various cell types. In squid giant axons, hyperpolarization induces a calcium influx from the extracellular medium (Hallett and Carbone, 1972). In rat mast cells, secretory stimulation leads to a large $[Ca^{2+}]_i$ transient followed by a plateau of elevated $[Ca^{2+}]_i$, which is increased with hyperpolarization (Penner et al., 1988). In stimulated *Xenopus* oocytes, hyperpolarization enhances Ca^{2+} influx, and this accelerates intracellular calcium waves (Girard and Clapham, 1993). Hence Ca^{2+} entry at the hyperpolarized side can be due to the enhanced driving force. Consistent with this, Ca^{2+} enters this side of the cell near the peak of the pulse when the cell is strongly hyperpolarized.

Nucleation of waves at the depolarized side of the cells implicates a different sequence of events. Nucleation was delayed with respect to the hyperpolarized side, but wave propagation occurred at similar speeds. Ca^{2+} influx could occur through the sodium-calcium exchanger; normally Ca^{2+} is extruded while Na^+ enters the cell, but when the membrane potential is depolarized, Ca^{2+} enters the cell while Na^+ is extruded. This influx may again be amplified by Ca^{2+}-activated nonselective cation channels permeable to Ca^{2+}.

Wave propagation

Once Ca^{2+} enters the cell, it can induce Ca^{2+} release from intracellular stores if it reaches a threshold concentration. Waves did not propagate in thapsigargin-treated cells, showing that intracellular release is necessary for propagation. This agrees with results in frog eggs, which can be prick-activated in a Ca^{2+}-containing medium. Calcium-induced calcium release is stimulated by entry of extracellular Ca^{2+} through the wound (Cheer et al., 1987).

Cells can have two types of calcium stores, inositol trisphosphate (IP_3)-sensitive stores and ryanodine-sensitive stores. The latter are primarily found in excitable cells (Meyer and Stryer, 1991), whereas most cells have at least one form of IP_3 receptor (Marks, 1997). Fish keratocytes, nonexcitable cells, are likely to have IP_3-sensitive stores and no ryanodine-sensitive stores. This is supported by our observation that up to 50 mM caffeine, which often releases Ca^{2+} from ryanodine stores, had no effect on $[Ca^{2+}]_i$, although we cannot exclude the possibility of ryanodine-sensitive, caffeine-insensitive stores.

IP_3-sensitive stores release Ca^{2+} in response to an increase in Ca^{2+} or in IP_3 (Berridge, 1993), which is, in turn, produced in response to Ca^{2+}. Thus Ca^{2+} can amplify its own release, generating a Ca^{2+} wave. In some cell types, it has been found that IP_3 alone can mediate Ca^{2+} waves and oscillations; for example, in fertilized hamster eggs, Ca^{2+} release is mediated solely by the IP_3 receptor, and Ca^{2+}-sensitized IP_3-induced Ca^{2+} release generates $[Ca^{2+}]_i$ waves and oscillations (Miyazaki et al., 1992). In addition, mathematical models have shown that oscillations can occur even at a fixed IP_3 concentration (Atri et al., 1993; De Young and Keizer, 1992).

$[Ca^{2+}]_i$ decreased quickly. Some Ca^{2+} is pumped out of the cell, because $[Ca^{2+}]_i$ also decreases in thapsigargin-treated cells. In untreated cells it is probably also pumped back into stores. Subsequently, cells exhibited quasi-periodic oscillations; a possible mechanism involves Ca^{2+} influx through depletion-activated Ca^{2+} channels and propagation through induced Ca^{2+} release from intracellular stores. These oscillations persist for a long time after stimulation, indicating a persistent effect of the applied voltage pulse.

Model for wave generation

A general model for second messenger propagation has been described by Meyer (1991). In this model, a stimulus triggers a local increase in the concentration of messenger molecules. These diffuse into neighboring regions; if a threshold concentration is reached, more molecules will be produced. The process is thus self-propagating. To simplify the amplification process a model limit cycle amplifier is postulated: if the messenger concentration reaches a threshold concentration (C_{thr}), the amplifier increases the messenger concentration to its maximum level (C_{max}) after an intrinsic delay time (t_α). The wave generation parameters are t_α, $\alpha = \log(C_{max}/C_{thr})$, and the diffusion coefficient D. The experimentally measurable parameters are the velocity of wave propagation v and the rise time τ. These parameters are related by

$$v = \sqrt{D/\tau} \tag{1}$$

$$t_\alpha = \alpha\tau \tag{2}$$

A similar relationship (the velocity differs by a factor of order 1) has been proposed by Jaffe (1991) for reaction/diffusion waves. This is a very simple and incomplete model; other processes in the generation of calcium waves can be incorporated into a more complete model. However, as shown below, our results are consistent with this simplified model, which allows us to calculate a diffusion coefficient.

We applied this model to the voltage pulse-induced waves. Waves start with calcium entry through the plasma membrane, calcium diffuses to neighboring regions and, if it reaches a threshold concentration, induces calcium release from intracellular stores and possibly further Ca^{2+} entry through Ca^{2+}-activated nonselective cation channels permeable to Ca^{2+}. The threshold concentration, estimated from cases where a wave was not propagated (Fig. 2 *A*), was $\sim$1 μM. The maximum concentration reached was at least 3 μM; thus $\alpha \approx 0.5$. The average velocity through the cell body for waves propagating from the hyperpolarized side was $\sim 66 \pm 40$ μm/s (it was approximately the same for waves propagating from the depolarized side, but there were fewer waves). The rise time was estimated to be $\sim 68 \pm 23$

ms. Using Eq. 1, the diffusion coefficient is $D \approx 300 \pm 138$ $\mu m^2/s$, and from Eq. 2, $t_\alpha \approx 34$ ms.

This diffusion coefficient corresponds to the propagating molecule. Measurements of the diffusion coefficient of calcium ions vary between tens and hundreds of $\mu m^2/s$. Allbritton et al. (1992) reported a diffusion coefficient of 223 $\mu m^2/s$ for free ions, but a much lower number for buffered Ca^{2+} in a cytosolic extract from *Xenopus laevis* oocytes. Alternatively, the propagating molecule could be IP_3; its diffusion coefficient in *Xenopus laevis* oocytes extracts was 283 $\mu m^2/s$ (Allbritton et al., 1992). Comparison of these measurements with the diffusion coefficient calculated from the observed waves suggests that the propagating molecule is IP_3.

The delay time t_α is the time it takes the amplifier to respond once the threshold concentration has been reached. The amplification mechanism in the cell body is mainly calcium release; t_α is thus the time it takes the stores to release calcium. An independent measurement of this time would provide a test of this model.

CONCLUSIONS

Applied electric field pulses induce fast calcium waves in electrotactic fish keratocytes. Waves start with calcium influx through calcium channels in the plasma membrane, and if $[Ca^{2+}]_i$ reaches a threshold concentration, waves are propagated by the stimulation of Ca^{2+} release from intracellular stores and possibly by activation of nonselective cation channels in the plasma membrane. Subsequently, cells exhibit spontaneous spiking. Waves are induced if the imposed voltage drop across the cell is large enough (>150 mV), and propagate with velocities of 30–100 μm/s. The measured parameters are consistent with an amplification model that predicts the diffusion coefficient of the propagating molecule to be ~300 $\mu m^2/s$.

Cells show no apparent damage, they do not change shape, and they are still motile and electrotactic. As in the presence of small steady electric fields, cells align toward the cathode after repeated pulses. We do not detect calcium influx when cells are subjected to the small DC fields, but $[Ca^{2+}]_i$ changes are detected when cells reorient in both the presence and absence of the applied field (Brust-Mascher et al., 1994, 1995, and manuscript in preparation). These results, taken together, suggest that calcium influx may play a role in redirecting cells toward the cathode.

We thank Rebecca M. Williams and Dr. Warren Zipfel for technical assistance and Kevin Hodgson for help in the preparation of figures.

This research was supported by the National Institutes of Health (P41RR04224) and the National Science Foundation (NSF) (DIR8800278) and was carried out in the National Institutes of Health-NSF Developmental Resource for Biophysical Imaging and Optoelectronics. IB-M was supported by a predoctoral training grant from the National Institutes of Health (T32GM08267).

REFERENCES

Allbritton, N. L., T. Meyer, and L. Stryer. 1992. Range of messenger action of calcium ion and inositol 1,4,5-trisphosphate. *Science.* 258: 1812–1815.

Atri, A., J. Amundson, D. Clapham, and J. Sneyd. 1993. A single-pool model for intracellular calcium oscillations and waves in the *Xenopus laevis* oocyte. *Biophys. J.* 65:1727–1739.

Bassani, J. W. M., R. A. Bassani, and D. M. Bers. 1995. Calibration of indo-1 and resting intracellular $[Ca^{2+}]_i$ in intact rabbit cardiac myocytes. *Biophys. J.* 68:1453–1460.

Berridge, M. J. 1993. Inositol trisphosphate and calcium signalling. *Nature.* 316:315–325.

Blatter, L. A., and W. G. Wier. 1990. Intracellular diffusion, binding, and compartmentalization of the fluorescent calcium indicators indo-1 and fura-2. *Biophys. J.* 58:1491–1499.

Bray, D. 1992. Cell Movements. Garland Publishing, New York and London.

Brown, M. J., and L. M. Loew. 1994. Electric field-directed fibroblast locomotion involves cell surface molecular reorganization and is calcium independent. *J. Cell Biol.* 127:117–128.

Brundage, R. A., K. E. Fogarty, R. A. Tuft, and F. S. Fay. 1991. Calcium gradients underlying polarization and chemotaxis of eosinophils. *Science.* 254:703–706.

Brundage, R. A., K. E. Fogarty, R. A. Tuft, and F. S. Fay. 1993. Chemotaxis of newt eosinophils: calcium regulation of chemotactic response. *Am. J. Physiol.* 265:C1527–C1543.

Brust-Mascher, I., R. M. Williams, and W. W. Webb. 1994. Calcium distributions in motile electrotactic fish keratocytes measured by two-photon excited fluorescence microscopy. *Biophys. J.* 66:A411.

Brust-Mascher, I., R. M. Williams, and W. W. Webb. 1995. Calcium heterogeneities in fish keratocytes turning in electric fields. *Biophys. J.* 68:A282.

Cheer, A., J. P. Vincent, R. Nuccitelli, and G. Oster. 1987. Cortical activity in vertebrate eggs. I. The activation waves. *J. Theor. Biol.* 124:377–404.

Clapham, D. E. 1995. Calcium signaling. *Cell.* 80:259–268.

Cooper, M. S., and M. Schliwa. 1985. Electrical and ionic controls of tissue cell locomotion in DC electric fields. *J. Neurosci. Res.* 13:223–244.

Cooper, M. S., and M. Schliwa. 1986. Motility of cultured fish epidermal cells in the presence and absence of direct current electric fields. *J. Cell Biol.* 102:1384–1399.

Denk, W., J. H. Strickler, and W. W. Webb. 1990. Two-photon laser scanning fluorescence microscopy. *Science.* 248:73–76.

De Young, G. W., and J. Keizer. 1992. A single-pool inositol 1,4,5-trisphospate-receptor-based model for agonist-stimulated oscillations in Ca^{2+} concentration. *Proc. Natl. Acad. Sci. USA.* 89:9895–9899.

Feder, T. J., and W. W. Webb. 1994. Redistribution of plasma membrane proteins by electroosmosis elicits cytosolic calcium response in tumor mast cells. *J. Cell. Physiol.* 161:227–236.

Fewtrell, C. 1993. Ca^{2+} oscillations in non-excitable cells. *Annu. Rev. Physiol.* 55:427–454.

Forscher, P. 1989. Calcium and polyphosphoinositide control of cytoskeletal dynamics. *Trends Neurosci.* 12:468–474.

Ghosh, P. M., C. R. Keese, and I. Giaever. 1993. Monitoring electropermeabilization in the plasma membrane of adherent mammalian cells. *Biophys. J.* 64:1602–1609.

Girard, S., and D. Clapham. 1993. Acceleration of intracellular calcium waves in *Xenopus* oocytes by calcium influx. *Science.* 260:229–232.

Gross, D., L. M. Loew, and W. W. Webb. 1986. Optical imaging of cell membrane potential. Changes induced by applied electric fields. *Biophys. J.* 50:339–348.

Grynkiewicz, G., M. Poenie, and R. Y. Tsien. 1985. A new generation of Ca^{2+} indicators with greatly improved fluorescence properties. *J. Biol. Chem.* 260:3440–3450.

Hahn, K., R. DeBiasio, and D. L. Taylor. 1992. Patterns of elevated free calcium and calmodulin activation in living cells. *Nature.* 359:736–738.

Hallett, M., and E. Carbone. 1972. Studies of calcium influx into squid giant axons with aequorin. *J. Cell Physiol.* 80:219–226.

Hendey, B., and F. R. Maxfield. 1993. Regulation of neutrophil motility and adhesion by intracellular calcium transients. *Blood Cells.* 19: 143–164.

Hove-Madsen, L., and D. M. Bers. 1992. Indo-1 binding to protein in permeabilized ventricular myocytes alters its spectral and Ca binding properties. *Biophys. J.* 63:89–97.

Jaffe, L. F. 1991. The path of calcium in cytosolic calcium oscillations: a unifying hypothesis. *Proc. Natl. Acad. Sci. USA.* 88:9883–9887.

Janmey, P. A. 1994. Phosphoinositides and calcium as regulators of cellular actin assembly and disassembly. *Annu. Rev. Physiol.* 56:169–191.

Lückhoff, A., and D. E. Clapham. 1994. Calcium channels activated by depletion of internal calcium stores in A431 cells. *Biophys. J.* 67: 177–182.

Marks, A. R. 1997. Intracellular calcium-release channels: regulators of cell life and death. *Am. J. Physiol.* 272:H597–H605.

Marks, P. W., B. Hendey, and F. R. Maxfield. 1991. Attachment to fibronection or vitronectin makes human neutrophil migration sensitive to alterations in cytosolic free calcium concentration. *J. Cell Biol.* 112:149–158.

Marks, P. W., and F. R. Maxfield. 1990. Transient increases in cytosolic free calcium appear to be required for the migration of adherent human neutrophils. *J. Cell Biol.* 110:43–52.

Maxfield, F. R. 1993. Regulation of leukocyte locomotion by Ca^{2+}. *Trends Cell Biol.* 3:386–391.

McCloskey, M. A., Z-Y. Liu, amd M-M. Poo. 1984. Lateral electromigration and diffusion of Fc_ϵ receptors on rat basophilic leukemia cell: effects of IgE binding. *J. Cell Biol.* 99:778–787.

Meyer, T. 1991. Cell signaling by second messenger waves. *Cell.* 64: 675–678.

Meyer, T., and L. Stryer. 1991. Calcium spiking. *Annu. Rev. Biophys. Biophys. Chem.* 20:153–174.

Mittal, A. K., and J. Bereiter-Hahn. 1985. Ionic control of locomotion and shape of epithelial cells. I. Role of calcium influx. *Cell Motil.* 5:123–136.

Miyazaki, S., M. Yuzaki, K. Nakada, H. Shirakawa, S. Nakanishi, S. Nakade, and K. Mikoshiba. 1992. Block of Ca^{2+} wave and Ca^{2+} oscillation by antibody to the inositol 1,4,5-trisphosphate receptor in fertilized hamster eggs. *Science.* 257:251–255.

Mullins, R. D., J. E. Sisken, and B. F. Sisken. 1992. Extremely low frequency sinusoidal electric fields mobilize calcium from an intracellular store in Swiss 3T3 fibroblasts in a frequency and amplitude dependent manner. Presented at the Annual Meeting of the American Society for Cell Biology, Denver, CO.

Nishimura, K. Y., R. R. Isseroff, and R. Nuccitelli. 1996. Human keratinocytes migrate towards the negative pole in direct current electric fields comparable to those measured in mammalian wounds. *J. Cell Sci.* 109:199–207.

Nuccitelli, R. 1988. Physiological electric fields can influence cell motility, growth and polarity. *Adv. Cell Biol.* 2:213–233.

Onuma, E. K., and S. W. Hui. 1988. Electric field-directed cell shape changes, displacement, and cytoskeletal reorganization are calcium dependent. *J. Cell Biol.* 106:2067–2075.

Parekh, A., H. Teriau, and W. Stühmer. 1993. Depletion of $InsP_3$ stores activates a Ca^{2+} and K^+ current by means of a phosphatase and a diffusible messenger. *Nature.* 364:814–818.

Penner, R., G. Matthews, and E. Neher. 1988. Regulation of calcium influx by second messengers in rat mast cells. *Nature.* 11:499–504.

Piston, D. W., M. S. Kirby, H. Cheng, W. J. Lederer, and W. W. Webb. 1994. Two-photon-excitation fluorescence imaging of three-dimensional calcium-ion activity. *Appl. Optics.* 33:662–669.

Poo, M-M. 1981. In situ electrophoresis of membrane components. *Annu. Rev. Biophys. Bioeng.* 10:245–276.

Prausnitz, M. R., C. D. Milano, J. A. Gimm, R. Langer, and J. C. Weaver. 1994. Quantitative study of molecular transport due to electroporation: uptake of bovine serum albumin by erythrocyte ghosts. *Biophys. J.* 66:1522–1530.

Putney, J. W. 1990. Capacitative calcium entry revisited. *Cell Calcium.* 11:611–624.

Randriamampita, C., and R. Y. Tsien. 1993. Emptying of intracellular Ca^{2+} stores releases a novel small messenger that stimulates Ca^{2+} influx. *Nature.* 364:809–814.

Robinson, K. R. 1985. The responses of cells to electrical fields: a review. *J. Cell Biol.* 101:2023–2027.

Stossel, T. P. 1989. From signal to pseudopod: how cells control cytoplasmic actin assembly. *J. Biol. Chem.* 264:18261–18264.

Thastrup, O., P. J. Cullen, B. K. Drobak, M. R. Hanley, A. P. Dawson. 1990. Thapsigargin, a tumor promoter, discharges intracellular Ca^{2+} stores by specific inhibition of the endoplasmic reticulum Ca^{2+}-ATPase. *Proc. Natl. Acad. Sci. USA.* 87:2466–2470.

Tsien, R. W., and R. Y. Tsien. 1990. Calcium channels, stores, and oscillations. *Annu. Rev. Cell Biol.* 6:715–760.

von Tscharner, V., B. Prod'hom, M. Baggiolini, and H. Reuter. 1986. Ion channels in human neutrophils activated by a rise in free cytosolic calcium concentration. *Nature.* 324:369–372.

Weeds, A. 1982. Actin-binding proteins—regulators of cell architecture and motility. *Nature.* 296:811–816.

Williams, R. M., D. W. Piston, and W. W. Webb. 1994. Two-photon molecular excitation provides intrinsic 3-dimensional resolution for laser-based microscopy and microphotochemistry. *FASEB J.* 8:804–813.

Zimmermann, U. 1982. Electric field-mediated fusion and related electrical phenomena. *Biochim. Biophys. Acta.* 694:227–277.